KJO
pISSN: 1011-8942 eISSN: 2092-9382

Korean J Ophthalmol 2010;24(2):108-118
DOI: 10.3341/kjo.2010.24.2.108

Original Article

Retinal Protective Effects of Resveratrol via Modulation of Nitric Oxide Synthase on Oxygen-induced Retinopathy

Woo Taek Kim[1], Eok Soo Suh[2]

[1]*Department of Pediatrics, Catholic University of Daegu School of Medicine, Daegu, Korea*
[2]*Department of Ophthalmology, Dongguk University College of Medicine, Gyeongju, Korea*

Purpose: Retinopathy of prematurity (ROP) is one of the leading causes of blindness, with retinal detachment occurring due to oxygen toxicity in preterm infants. Recently, advances in neonatal care have led to improved survival rates for preterm infants, and ROP has increased in incidence. In the present study, we aimed to determine whether or not resveratrol exhibits protective effects in an animal model of ROP and in primary retinal cell cultures of neonatal rat via nitric oxide (NO)-modulating actions using western blotting and real-time PCR with inducible nitric oxide synthase (iNOS), endothelial NOS (eNOS) and neuronal NOS (nNOS) antibodies and mRNAs.

Methods: In an *in vivo* oxygen-induced retinopathy (OIR) model, cyclic hyperoxia was induced with 80% O_2 for one day and 21% O_2 for one day from P1 to P14 in newborn Sprague-Dawley (SD) rats. Resveratrol was injected intravitreally for seven days and rats were sacrificed at P21. *In vitro* OIR primary retinal cell culture was performed using P0-2 SD rats. Hyperoxia injuries were induced through 100% O_2 exposure for six hours. Western blotting and real-time PCR using iNOS, eNOS, nNOS antibodies and primers were performed in the rat model of ROP and the dispersed retinal cell culture.

Results: In both *in vivo* and *in vitro* OIR, the expression of iNOS antibody and mRNA was increased and of eNOS and nNOS were reduced in the resveratrol-treated group.

Conclusions: In conclusion, resveratrol appeared to exert retinal protective effects via modulation of NO-mediated mechanism in *in vivo* and *in vitro* OIR models.

Key Words: Nitric oxide synthase, Retinopathy of prematurity, Resveratrol

Retinopathy of prematurity (ROP) is a leading cause of blindness and a complex disease of the immature retina in premature infants. This disease affects approximately 80% of babies born with birthweights less than 1000 g [1]. Preservation of visual acuity in ROP usually requires ablation of the peripheral retina via methods such as cryotherapy and laser photocoagulation therapy [2]. Because of these treatments the incidence of blindness was reduced by 25%. Clinical manifestations of ROP range from mild transient changes of the peripheral retina to severe progressive vasoproliferation resulting in scarring, retinal detachment, and potential blindness. ROP includes all stages of disease such as acute (early) or chronic (late or cicatricial) stages, as well as late sequelae such as high myopia, strabismus, amblopia, diplopia, glaucoma, cataract, viterous hemorrhage, and low vision [3]. Retrolental fibroplasia (RLF), the previous name for this disease, describes only the cicatricial stages. Given the current understanding of ROP, it is recommended that all infants born at less than 1500 g receive regular eye examinations starting at four weeks chronologic age or 31 weeks postconceptional age, whichever is later [4].

After premature delivery, oxygen levels in postnatal tissue are significantly increased compared to those *in utero*. Additionally, oxygen therapy further increases oxygen levels in the developing retina. This hyperoxia results in vaso-obliteration and destruction of normal retinal vascular development. At that time, low insulin-like growth factor (IGF)-1 levels decrease and hypoxia inducible factor (HIF), as transcriptional factor for vascular endothelial growth factor (VEGF), and VEGF are also reduced. After the return to

Received: June 19, 2009 *Accepted*: March 5, 2010

Reprint requests to Eok Soo Suh. Department of Ophthalmology, Dongguk University College of Medicine, #1090-1 Seokjang-dong, Gyeongju 780-714, Korea. Tel: 82-54-770-8566, Fax: 82-54-772-9618, E-mail: suksu@dongguk.ac.kr

normal oxygen levels after the cessation of oxygen therapy, the nonperfused portions of the retina become hypoxic. Retinal hypoxia stimulates IGF-1, HIF, and VEGF before neovascularization. VEGF causes retinal neovascularization and retinal proliferation. VEGF results in extraretinal angiogenesis–stage 3 ROP at the vitreoretinal interface of the ROP ridge. Stage 3 ROP may resolve spontaneously, or may progress to traction retinal detachment and blindness. Further inhibition of IGF-1, HIF, and VEGF decreases retinal neovascularization [5].

In the present study, an *in vivo* oxygen-induced retinopathy (OIR) model was designed using a rat model of ROP induced by cyclic hyperoxia, exposed to 80% O_2 for one day and 21% O_2 for another day from P1 to P14 of newborn Sprague-Dawley (SD) rats, as described by Penn et al. [6] Retinal detachment was identified using Hematoxylin and eosin (H&E) staining. An *in vitro* OIR model was designed using dispersed retinal cell cultures, as described by Seigel [7]. All cells were damaged by oxygen exposure for six hours. Photoreceptors, the major population of neuronal cells in retinal cell culture, were immunolabeled with interphotoreceptor retinoid-binding protein (IRBP) antibody.

Resveratrol (trans-3,5,4'-trihydroxystilbene) is a phytoalexin produced by a variety of plants such as grapes, peanuts, and berries in response to stress, injury, ultraviolet irradiation, and fungal infection [8]. Resveratrol can be detected in the leaf epidermis and the skin of grapes [9]. The "French paradox," the low incidence of coronary heart diseases in spite of a diet rich in saturated fats has been attributed to a number of contained polyphenols, including resveratrol [10]. Resveratrol has some physiological effects, including prevention of lipid peroxidation in human LDL [11], inhibition of arachidonate acid metabolism [12], inhibition of platelet activity [13], and stimulation of NO production in endothelial cells to exert vasodilatory effect on blood vessels [14].

We investigated resveratrol as a nitric oxide (NO)-mechanism modulator to evaluate the mechanisms of ROP based on molecular biology and pharmacological treatments in the *in vivo* OIR model, the rat model of ROP, and the *in vitro* OIR model, the hyperoxic injury of cultured dispersed retinal cells. Recent reports reveal that retinal damage also occurs via NO-mediated mechanisms. Previously, we recognized that resveratrol exhibits neuroprotective effects and cardioprotective effects via modulation of NO-mediated mechanisms [15,16].

In the present study, the protective ability of resveratrol was explored in an animal model of ROP and in primary retinal cell cultures of neonatal rat retinas. We attempted to better define whether resveratrol is a promising treatment of ROP and has preventive mechanisms via NO-modulating actions using western blotting and real-time PCR with inducible nitric oxide synthase (iNOS), endothelial NOS (eNOS) and neuronal NOS (nNOS) antibodies and mRNAs.

Materials and Methods

Materials

Resveratrol, papain, glucose, and poly-*D*-lysine were purchased from Sigma (Sigma-Aldrich, St. Louis, MO, USA). Rabbit polyclonal IRBP and secondary goat anti-mouse or rabbit IgG-HRP antibodies were purchased from Santa Cruz Biotechnology (Santa Cruz, CA, USA). Rabbit polyclonal iNOS, rabbit polyclonal eNOS, and rabbit polyclonal nNOS antibodies were purchased from Assay Designs (Stressgen, Ann Arbor, MI, USA). 3-(4,5-dimethylthiazol-2-yl)-2,5-diphenyl-tetrazolium bromide (MTT) was purchased from Duchefa (Haarlem, Amsterdam, Netherlands). Hanks' balanced salt solution (HBSS), Eagle's Minimal Essential Medium (MEM), fetal bovine serum (FBS), and gentamicin were purchased from Gibco BRL (Grand Island, NY, USA). DNase I was obtained from Takara (Otsu, Shiga, Japan). Complete protease inhibitor cocktail tablets were purchased from Roche Applied Science (Mannheim, Germany). Enhanced chemiluminoscence (ECL) and a western blotting detection system were purchased from Amersham Biosciences (Piscataway, NJ, USA). SUPEX was purchased from Neuronex (Pohang, Korea).

Animal model of ROP (*in vivo* OIR)

Postnatal day 1 SD rats were obtained from Samtako (Osan, Korea) or HyoChang Science (Daegu, Korea). We implemented a cyclic oxygen exposure protocol that was modified from previous rat oxygen-induced retinopathy studies [6]. Hyperoxic experiments were conducted in an airtight polypropylene container 295×230×84 mm (3.9 L volume; Lock & Lock, Yongin, Korea) equipped with inlet and outlet ports. The inlet port received 100% medical grade oxygen and the airflow from the outlet was monitored for oxygen content using an oxygen monitor (Hudson RCI, Temecula, NC, USA). The oxygen levels remained above 98% throughout the entire exposure period. The interior of the chamber was maintained at room temperature. Control animals were maintained in room air. The cyclic hyperoxic conditions were performed at 80% O_2 for one day and 21% O_2 for another day from P1 to P14 in newborn SD rats. The drug was injected intravitreally (into the vitreous humour of the eye) once a day for seven days and the rats were sacrificed at P21.

The animals were divided into three groups. Group 1 (normoxia control, N, n=7) was not exposed to hyperoxia. Group 2 (hyperoxia only, H, n=8) was subjected to hyperoxia without treatment. Group 3 (hyerpoxia+resveratrol, HR, n=8) was administered resveratrol (30 mg/kg, intraperitoneal injection).

H&E stain

Histologic studies were performed seven days after hyperoxic insult. After sacrifice and intracardiac perfusion

with saline, the rats' eyes were removed, fixed in 4% paraformaldehyde, embedded in paraffin, and prepared for light microscopy. Four μm sections were mounted on glass slides. Sections were deparaffinized in xylene for 30 minutes and serially treated with 100% (5 minutes), 96% (10 minutes), and 70% (10 minutes) ethanol. Slides were stained with hematoxylin, rinsed for a few seconds with water to remove excess stain, placed in 1% eosin, then rinsed again briefly in water to remove the acid and washed through a successive series of 70%, 95%, and 100% ethanol at five minutes each. Finally, the slides were transferred to xylene for clearing, mounted, and cover slipped.

Primary culture of dissociated-dispersed retinal cells (*in vitro* OIR)

This study was performed in accordance with the approved animal use guidelines of the Catholic University of Daegu. Primary retinal tissue was obtained from postnatal 0-2 day SD rats. Retinal cell cultures were prepared using rat eyes as described [7]. The rats were anesthetized with ether and the eyes were removed. Under a stereomicroscope, the neuroretinas were carefully dissected free from the pigmented epithelium and optic nerve, and placed in HBSS. Tissues were cut into 2×2×2 mm sizes with a knife, transferred into 2 mL of papain in a conical tube, and incubated for 40 minutes at 37℃. After incubation, the cells were added to Eagle's MEM containing 3 mL FBS, 0.1 mL 0.2% DNase I, and pipetted 20 times with a pasteur pipette. Cells were centrifuged at 1000 rpm for 8 minutes, the supernatant was decanted, and the cell pellets were resuspended in 3 mL medium and centrifuged again at 1000 rpm for 8 minutes. The pellets were resuspended in 2 mL medium and the cells were plated in 24-well tissue culture plates on 12 mm coverslips or 10 cm dishes that had been pre-treated overnight with poly-*D*-lysine (100 ug/mL). The cells were maintained in Eagle's MEM with 10% FBS, 10% glucose, and 2 mg/mL gentamicin.

The cultured cells were divided into three groups: normoxia (N), hyperoxia (H), and hyperoxia+resveratrol (5 ug/mL, HR). The N group was placed in a 5% CO_2 incubator, and the H and the HR groups were placed in a 5% CO_2 incubator with 100% O_2 for 6 hours. All groups except the N group were treated with drugs before hyperoxic insult.

MTT assay

The MTT assay was used to estimate cell viability and growth as originally described by Mosmann [17]. MTT was dissolved at a concentration of 5 mg/mL. Ten μL of the 5 mg/mL MTT stock solution was added to each well. After four hours of incubation at 37℃, the media were removed and 100 μL of lysing buffer (dimethyl sulfoxide, DMSO; 95% ethanol=1:1) was added. Absorbance of the samples was read at 492 nm using a microtiter plate enzyme-linked immunosorbent assay (ELISA) reader. The amount of formazan produced was proportional to the number of live and metabolically active cells.

Immunofluorescence assays

To measure immunofluorescence (IF), cultured cells were first washed twice with PBS and fixed with 4% paraformaldehyde at 4℃ for 30 minutes. The cells were washed twice more with 1×PBS and incubated with 1% BSA at room temperature for one hour. The cells were then incubated with IRBP antibody for two hours and washed three times with PBS. Washed cells were treated with fluorescence-conjugated secondary antibodies for one hour.

Rat retinal protein extraction

Pup rats of the *in vivo* OIR model were sacrificed at P21. The eyes were removed, eye cups were dissected, and anterior segments and neuroretina were detached, frozen in liquid nitrogen, and stored at -70℃ until further use. Frozen tissues were homogenized in protein lysis buffer containing complete protease inhibitor cocktail tablets, 1 M Tris-HCl (pH 8.0), 5 M NaCl, 10% Nonidet P-40, and 1 M 1,4-dithio-DL-threitol (DTT). After incubation for 20 minutes on ice, the samples were centrifuged at 12,000 rpm at 4℃ for 30 minutes and the supernatants were transferred to new tubes. Total proteins were measured with a Bio-Rad Bradford kit (Bio-Rad Laboratories, Hercules, CA, USA).

Sodium dodecyl sulfate-polyacrylamide gel electrophoresis (SDS-PAGE) and western blot analysis

Equal amounts of proteins (30 μg) were subjected to 6% or 12% SDS-PAGE after denaturing in 5×SDS gel-loading buffer (60 mM Tris-HCl pH 6.8, 25% glycerol, 2% SDS, 14.4 mM 2-mercaptoehanol, and 0.1% bromophenol blue) in boiling water for 10 minutes. After electrophoresis, proteins were electrotransferred to a polyvinylidene difluoride (PVDF) membrane (Millipore, Bedford, MA, USA) at a constant voltage of 10 V for 30 minutes. After transfer, the membrane was washed twice with 1×Tris-buffered saline (TBS) plus 0.1% Tween-20 (TBST, pH 7.4) and preincubated with a blocking buffer (5% nonfat dry milk in TBST) at room temperature for 1 hour. The blots were then incubated with rabbit polyclonal iNOS, rabbit polyclonal eNOS, and rabbit polyclonal nNOS primary antibodies at 1:1000 dilutions in TBST at 4℃ overnight. Following primary antibody incubations, the blots were incubated with secondary anti-rabbit or anti-mouse antibody (Santa Cruz Biotechnology) conjugated with horseradish peroxidase at 1:2000 dilution at room temperature for one hour. Finally, the membrane was washed and developed using ECL plus or SUPEX reagents. The intensities of the western blot bands were measured using a densitometer (Multi Gauge

Table 1. Primer pairs and annealing temperatures for real-time PCR

Name	Primer Sequence (5'-3')	Annealing (℃)	Amplicon size (bp)
iNOS	F: AGGCTTGGGTCTTGTTAGCCTAGT	55	270
iNOS	R: ATTCTGTGCAGTCCCAGTGAGGAA	55	270
eNOS	F: GGATTCTGGCAAGACCGATTAC	57	159
eNOS	R: GGTGAGGACTTGTCCAAACACT	57	159
nNOS	F: CCTTCCGAAGCTTCTGGCAACAGC	59	474
nNOS	R: TGGACTCAGATCTAAGGCGGTTGG	59	474

iNOS=inducible nitric oxide synthase; eNOS=endothelial nitric oxide synthase; nNOS=neuronal nitric oxide synthase.

Software; Fuji Photofilm, Tokyo, Japan).

RNA extraction and real-time PCR

Total RNA was extracted from tissue with TRIzol reagent (Invitrogen Corporation, Carlsbad, CA, USA). Briefly, total tissue or cells were homogenized in 1 mL of TRIzol reagent. Total RNA was separated from DNA and proteins by adding chloroform and was precipitated using isopropanol. The precipitate was washed twice in 100% ethanol, air-dried, and re-diluted in diethyplyrocarbonate (DEPC)-treated distilled water. The amount and purity of extracted RNA was quantitated by spectrophotometry (GeneQuant™ pro RNA/DNA calcular; GE Healthcare, Piscataway, NJ, USA), and the RNA was stored at -70℃ pending further processing. For reverse transcription, total RNA (2 μg) was reverse transcribed for one hour at 37℃ in a reaction mixture containing 20 U RNase inhibitor (Promega, Madison, WI, USA), 1 mM dNTP (Promega), 0.5 ng oligo-(dT) 15 primer (Promga), 1× ReT buffer and 200 U M-MLV reverse transcriptase (Promega). The reaction mixture was then incubated at 95℃ for five minutes to stop the reaction. The cDNA was stored at -20℃ until further processing.

Real-time PCR was performed in 48-well PCR plates (Mini Opticon™ Real-Time PCR System; Bio-Rad) using Finnzymes DyNAmo SYBR green qPCR kit (Finnzymes, Beverly, MA, USA). Amplification conditions are shown in Table 1. It was the same for all apoptotic and oxidant mRNA assayed: 95℃ for 15 minutes, followed by 40 cycles of 95℃ for 45 seconds, annealing temperature for 45 seconds, and 72℃ for 45 seconds. Real-time PCR data were analyzed with LightCycler software (Bio-Rad).

Statistical analysis

Data were expressed as mean±SD, analyzed by means of analysis of variance, and further assessed by Student's *t*-tests. $p<0.05$ were considered significant.

Results

Morphologic changes in the *in vivo* OIR model

The N group did not show any ocular pathology (Fig.

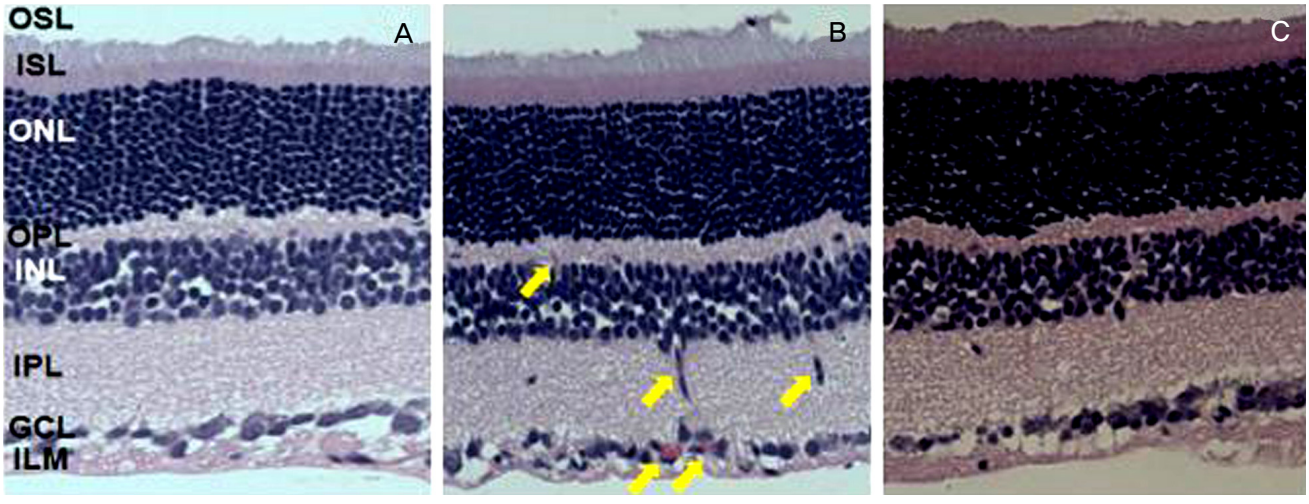

Fig. 1. Morphologic analysis after H&E staining revealed changes in the major retinal layers of 21-day-old Sprague-Dawley rats. (A) The N group did not show any retinal pathology. (B) In striking contrast, the H group presented retinal lesions displaying retinal neovascularization, fibrovascular growth, and large areas with blood vessel leakage like retinal detachment. (C) The HR group shows a few holes which are not retinal detachment. N=normoxia; H=hyperoxia; HR=hyperoxia+resveratrol; OSL=outer segment layer; ISL=inner segment layer; ONL=outer nuclear layer; OPL=outer plexiform layer; INL=inner nuclear layer; IPL=inner plexiform layer; GCL=ganglion cell layer; ILM=inner limiting membrane.

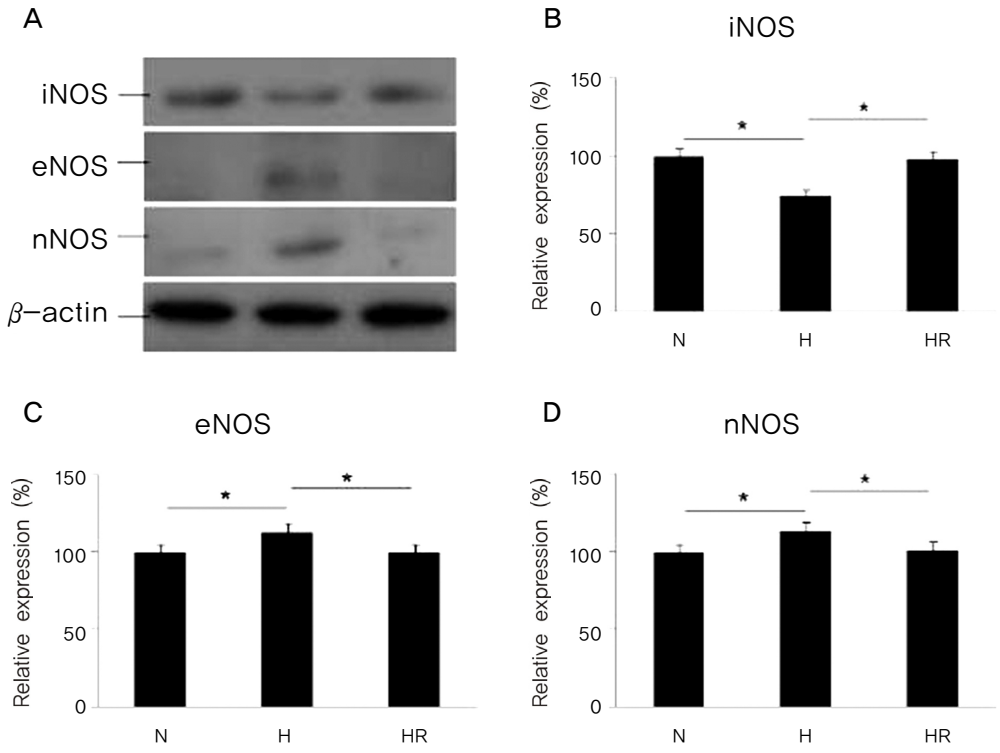

Fig. 2. (A)Western blots for inducible nitric oxide synthase (iNOS), endothelia nitric oxide synthase (eNOS), and neuronal nitric oxide synthase (nNOS) in the *in vivo* oxygen-induced retinopathy (OIR) were revealed. Relative expressions of iNOS (B), eNOS (C), and nNOS (D) in the N, H, and HR groups were revealed. The HR group was administered with 30 mg/kg of resveratrol before a hyperoxic insult. N=normoxia; H=hyperoxia; HR=hyperoxia+resveratrol. *$p<0.05$, statistically significant.

1A). In contrast, the H group had retinal lesions in the inner nuclear layer (INL), the ganglion cell layer (GCL), and the inner limiting membrane (ILM) retinal layers, displaying retinal neovascularization, fibrovascular growth, and large areas with blood vessel leakage, such as retinal detachment (Fig. 1B). In the HR group (Fig. 1C), a few holes were noted, but retinal detachments had subsided.

The expressions of iNOS, eNOS, and nNOS by western blot analysis in the *in vivo* OIR model

The expression of iNOS was reduced in the H group when compared to the N group, and was increased in the HR group when compared to the H group ($p<0.05$). In contrast, the expressions of eNOS and nNOS were increased in the H group compared to the N group, and were decreased in the HR group compared to the H group ($p<0.05$) (Fig. 2).

The expressions of iNOS, eNOS, and nNOS mRNA by real-time PCR analysis in the *in vivo* OIR model

The expression of iNOS mRNA was reduced in the H group compared to the N group, and was increased in the HR group compared to the H group ($p<0.05$). In contrast, the expressions of eNOS and nNOS mRNA were increased in the H group compared to the N group, and was decreased in the HR group compared to the H group ($p<0.05$) (Fig. 3).

Cell viability in the *in vitro* OIR model

By measuring the relative cell viability determined by the MTT assay in different concentrations, ranging from 5-100 ug/mL. the optimal concentration of resveratrol was 5 ug/mL, therefore, we used 5 ug/mL of resveratrol in the experiment (Fig. 4).

Morphologic changes from cell damage in the *in vitro* OIR

The cultured retinal cells were observed using fluorescence microscopy with photoreceptor marker, IRBP under high magnification (×200) (Fig. 5A). Cultured retinal cell growth was observed with a phase contrast microscope (×100). Cells in the N group (Fig. 5B) appeared normal, whereas cells in the H group (Fig. 5C) showed cellular swelling with indistinct nuclear shapes. Cells in the HR group (Fig. 5D) had a similar appearance to the N group.

The expressions of iNOS, eNOS, and nNOS by western blot analysis in the *in vitro* OIR

The expression of iNOS was reduced in the H group when compared to the N group, and was increased in the

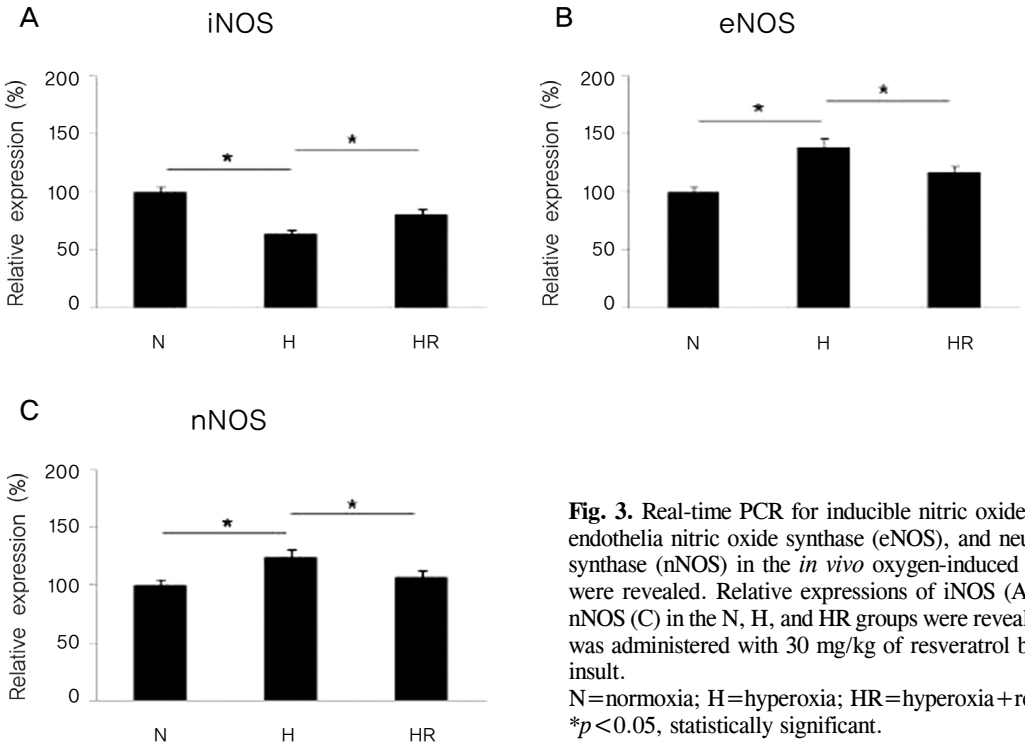

Fig. 3. Real-time PCR for inducible nitric oxide synthase (iNOS), endothelia nitric oxide synthase (eNOS), and neuronal nitric oxide synthase (nNOS) in the *in vivo* oxygen-induced retinopathy (OIR) were revealed. Relative expressions of iNOS (A), eNOS (B), and nNOS (C) in the N, H, and HR groups were revealed. The HR group was administered with 30 mg/kg of resveratrol before a hyperoxic insult.
N=normoxia; H=hyperoxia; HR=hyperoxia+resveratrol.
*$p<0.05$, statistically significant.

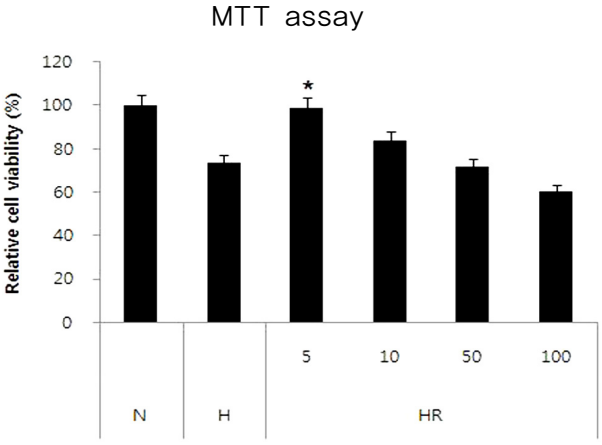

Fig. 4. Resveratrol attenuation in the *in vivo* oxygen-induced retinopathy (OIR). Cultured dispersed retinal cells were prepared with different concentrations of resveratrol for 30 min before hyperoxic insult for 6 hours. Cell viability was measured by the 3-(4,5-dimethylthiazol-2-yl)-2,5-diphenyl-tetrazolium bromide (MTT) assay. The concentrations of the drugs were 5, 10, 50 and 100 ug/mL.
N=normoxia; H=hyperoxia; HR=hyperoxia+resveratrol.
*$p<0.05$, statistically significant vs. N.

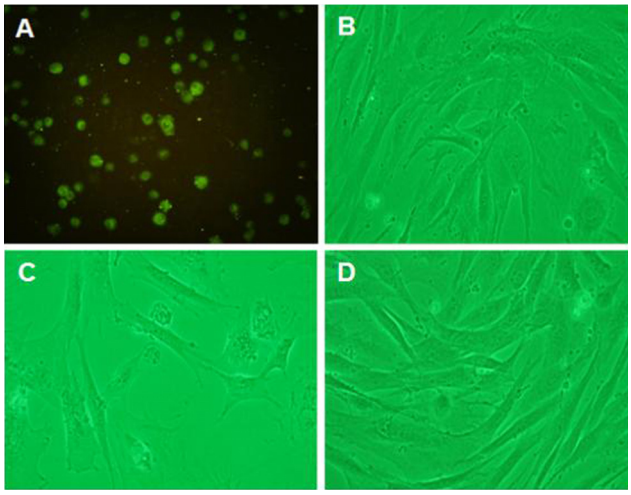

Fig. 5. (A) Immunofluorescence of photoreceptor marker IRBP (interphotoreceptor retinoid-binding protein) using a fluorescence microscope under high magnification (normoxia group, ×200), and photomicrographs of cultured dispersed retinal cells with a phase contrast microscope (×100). The N (B), H (C), and HR (D) groups were revealed. N=normoxia; H=hyperoxia; HR=hyperoxia+resveratrol.

HR group compared to the H group ($p<0.05$). In contrast, the expressions of eNOS and nNOS were increased in the H group compared to the N group, and were decreased in the HR group compared to the H group ($p<0.05$) (Fig. 6).

The expressions of iNOS, eNOS, and nNOS mRNA by real-time PCR analysis in the *in vitro* OIR

The expression of iNOS mRNA was reduced in the H group compared to the N group, and was increased in the HR group compared to the H group ($p<0.05$). In contrast, the expressions of eNOS and nNOS mRNA were increased in the H group compared to the N group, and were decreased in the HR group compared to the H group ($p<0.05$) (Fig. 7).

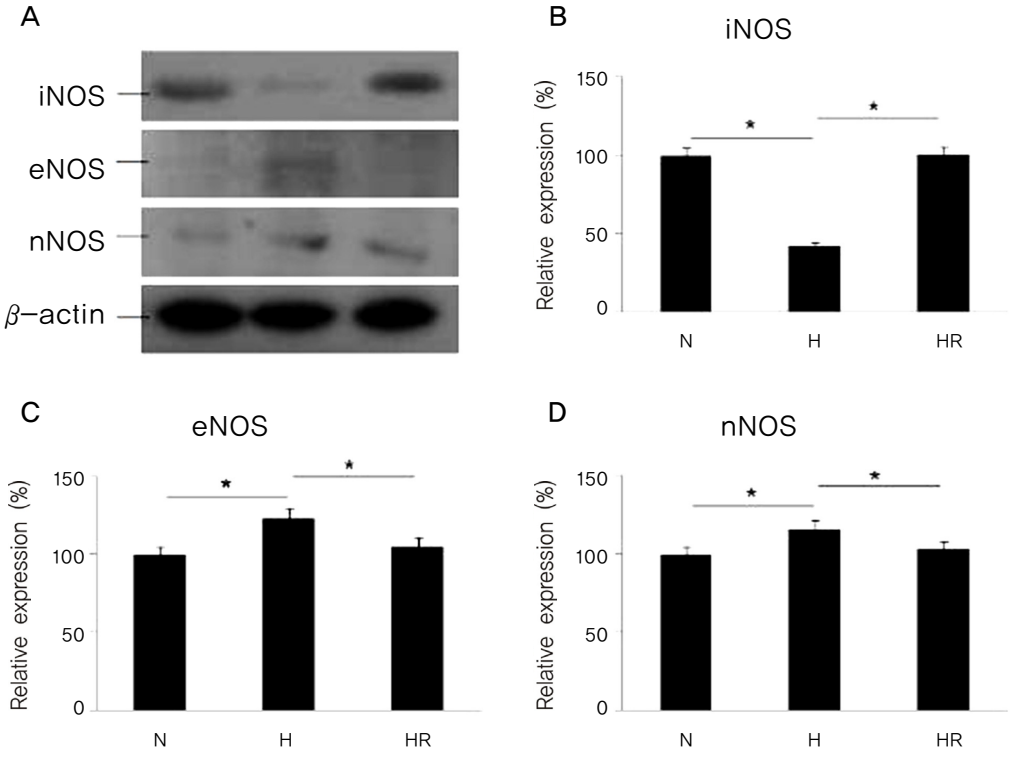

Fig. 6. (A) Western blots for inducible nitric oxide synthase (iNOS), endothelia nitric oxide synthase (eNOS), and neuronal nitric oxide synthase (nNOS) in the *in vitro* oxygen-induced retinopathy (OIR) were revealed. Relative expressions of iNOS (B), eNOS (C), and nNOS (D) in the N, H, and HR groups were revealed. The HR group was administered with 5 ug/mL of resveratrol before a hyperoxic insult. N=normoxia; H=hyperoxia; HR=hyperoxia+resveratrol. *$p<0.05$, statistically significant.

Discussion

ROP is a unique pattern of oxygen toxicity that can lead to retinal detachment and blindness in preterm infants who are born at less than 36 weeks of gestation. ROP was first described in 1942 (then termed RLF) as fibroblastic overgrowth of persistent vascular sheath behind each crystalline lens in extreme prematurity [18,19]. RLF was developed in preterm infants in 1949 [20]. Oxygen therapy became available in clinical practice and intensive oxygen therapy became known as a cause of RLF by 1952. In 1956, RLF was thought to develop in preterm infants after exposure to high concentrations of oxygen [21]. After the pathogenesis and clinical features of ROP became better understood, restricted oxygen therapy monitoring of oxygen levels lead to a dramatic decrease in the incidence of ROP. In the 1970s and 1980s, the development of techniques to continuously monitor oxygen, together with improved ventilators with better control of the inspired oxygen content, enabled arterial oxygen to be maintained within safe limits [22]. However, advances in neonatal care have to led improved survival rates in premature infants and concomitantly to increased incidence of ROP. Therefore, ROP has re-emerged as a significant clinical problem in premature infants [23].

ROP progresses in two phases, vasculogenesis and angiogenesis [24]. Phase I of ROP begins with delayed retinal vascular growth after birth and partial regression of existing vessels, i.e., vasculogenesis or the formation of blood vessels from endothelial precursor cells. By 14-15 weeks of gestational age, mesenchymal derived spindle cells grow into the superficial layer of the retina from the optic nerve. They migrate anteriorly, towards the retinal periphery and develop posteriorly, into primitive vascular tubes in which blood cells may be seen. They are not seen after 21 weeks of gestational age. Phase II of ROP begins with hypoxia-induced pathological vessel growth, i.e., angiogenesis or the development of new blood vessels by budding from existing blood vessels. From 17-18 weeks of gestational age, networks of capillaries form by angiogenesis and retinal vessels develop. From 25 weeks of gestational age, retinal capillaries have numerous arcades connecting arterial and venous vessels. VEGF is primarily secreted by retinal astrocytes and by Muller cells. Retinal astrocytes are closely associated with endothelial cells in the developing retinal vasculature. VEGF stimulates endothelial cell angiogenesis. Excessive oxygen contributes to ROP through regulation of VEGF. Suppression of VEGF by oxygen in phase I of ROP inhibits normal vessel growth, whereas elevated levels of VEGF induced by hypoxia in phase II of ROP precipitate pathological vessel proliferation. IGF-1 is a critical non-oxygen-regulated factor in ROP. The serum levels of IGF-1 in premature babies directly correlate with the severity of

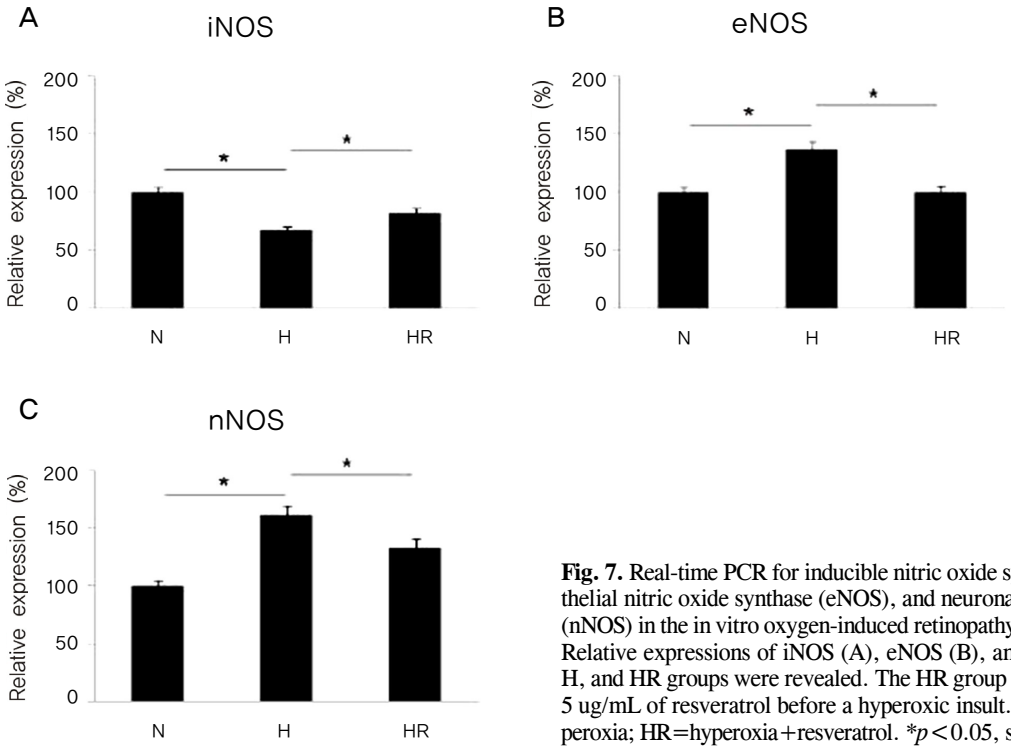

Fig. 7. Real-time PCR for inducible nitric oxide synthase (iNOS), endothelial nitric oxide synthase (eNOS), and neuronal nitric oxide synthase (nNOS) in the in vitro oxygen-induced retinopathy (OIR) were revealed. Relative expressions of iNOS (A), eNOS (B), and nNOS (C) in the N, H, and HR groups were revealed. The HR group was administered with 5 ug/mL of resveratrol before a hyperoxic insult. N=normoxia; H=hyperoxia; HR=hyperoxia+resveratrol. *$p < 0.05$, statistically significant.

clinical ROP. IGF-1 acts indirectly as a permissive factor by allowing maximal VEGF stimulation of vessel growth. Lack of IGF-1 in preterm infants prevents normal retinal vascular growth in phase I of ROP, despite the presence of VEGF. As infants mature, rising levels of IGF-1 in phase II of ROP allows VEGF stimulated pathological neovascularization. These findings suggest that restoration of IGF-1 to normal levels might be useful in preventing ROP in preterm infants. Angiogenesis appears to be driven by relative tissue hypoxia. HIF-1 is a nuclear protein that acts as a transcription factor for VEGF. HIF is rapidly degraded in normal tissue conditions, but the turnover time is prolonged in hypoxic conditions, leading to increased levels within the nucleus. Any postnatal factor that reduces HIF levels, such as the relative hyperoxia produced by oxygen therapy, will lead to reduced, and therefore delayed, angiogenisis-mediated retinal vascular development. At least one of the HIF proteins may be involved in the development of ROP [23,25,26].

Rat pups are immature at birth, and developmentally equivalent to a neonate born prematurely at 28 weeks postmenstrual age [23]. The first 14 days of a rat pup's life is equivalent to the period of 28 weeks to 40 weeks postmenstrual age in a human infant [23].

The pathogenesis of ROP was not well understood in early ROP animal models. Kitten models at that time were subjected to continuous high levels of oxygen. Retinal vasoobliteration occurred and when they returned to room air following exposure to oxygen, a vasoproliferative response was observed. However, these extreme conditions were not accurate models of clinical ROP [27]. A rat pup model was developed in order to better understand the pathogenesis of ROP using this information. The "Edinburgh" model oxygen paradigm consisted of a fluctuating oxygen profile derived from the case of an infant who developed stage 4 ROP. In a rat pup model, a fluctuating oxygen atmosphere alone could produce retinal vasculature abnormalities similar to those seen in clinical ROP. Thus, ROP may be explained in terms of exposure of the developing retinal vasculature to an abnormal oxygen environment. No other insult is necessary [28].

Retinal cell cultures were prepared using rat eyes as described by Seigel [7]. Since dispersed retinal cell cultures from postnatal rats are removed from the orderly structure of the intact retina, identification of these dispersed cells is paramount. In the dispersed rat embryonic retinal cell monolayer culture, flat cells and neuronal-like cells are evident, however, morphology alone is not enough to identify each of the six major phenotypes of the neuroretina: ganglion, bipolar, photoreceptor, amacrine, horizontal, and Müller cells. With the advent of retina specific antibodies, specific retinal cell types could be identified *in vitro* on the basis of retina-specific marker expression, rather than on less-reliable morphological characteristics [29].

Photoreceptor enrichment is also possible through the chemical destruction of undesired retinal neurons by the photoreceptor-sparing toxins kainic acid and ß-bungarotoxin [30] and by the non-ionic detergent Triton X-100 [31]. Mechanical selection through the adept use of a vibratome has been used as a physical means of photoreceptor purifi-

cation [32]. Retinal neurons have been shown to express proteins immunoreactive with glial markers (GFAP, S-100, and vimentin), photoreceptor markers (IRBP, S-Ag, recoverin), ganglion cell marker (2G12), as well as Müller cell marker (RetG1) [33]. Photoreceptors-immunolabeled with IRBP antibody-represented the major population of neuronal cells and consisted of approximately 65% rods and 35% cones (of total photoreceptors). In primary retinal cell cultures, the photoreceptors were mainly rods and represented the most abundant population in addition to Muller cells [34]. The MTT assay was used for estimation of cell viability and growth, as originally described by Mosmann [17].

To identify photoreceptors of retinal cells, the immunofluorescence assay photoreceptor marker, IRBP, was used. Cells in the N group appeared normal, whereas cells in the H group showed cellular swelling with indistinct nuclear shapes. Cells in the HR group had a similar appearance to those in the N group. Morphologically, damaged cells in the *in vitro* OIR were subsided according to administration of resveratrol.

NO, a cellular signaling molecule, is synthesized during the stoichiometric conversion of L-arginine to L-citrulline in the presence of oxygen and nicotinamide adenine dinucleotide phosphate (NADPH), which is catalyzed by nitric oxide synthase (NOS) [35]. NO inhibits platelet aggregation [36], inhibits platelets [37], and inhibits polymorphonuclear neutrophils [38]. NO is known as a vasodilator [39] and exerts a neuroprotective effect in stoke models [40]. Three isoforms of NOS that were named by the tissue are first cloned. Neuronal NOS (nNOS; 157 kDa) and endothelial NOS (eNOS; 140 kDa) are constitutively expressed and calcium-dependent, whereas inducible NOS (iNOS; 135 kDa) is expressed after immunologic challenge and neuronal injury, and is calcium-dependent under most circumstances. The eNOS and nNOS are present under physiological conditions, whereas iNOS is expressed in response to immunological stimulation. Additionally, eNOS produces NO with beneficial effects, such as vasodilative effect, antiplatelet aggregation effect, and inhibits PMN adhesion, whereas nNOS and iNOS produce NO with deleterious effects [41,42]. Generally, in the hypoxic injury of neurons, the expression of iNOS increased but those of eNOS and nNOS decreased. The expression of NOS isoforms after damage still remains controversal.

Resveratrol exhibits anti-inflammatory activity by inhibition of inflammatory mediators [43]. Resveratrol has anti-cancer activity and interferes with stages of carcinogenesis, including initiation, promotion, and progression [44]. Resveratrol also possesses antioxidant effects [45] and has anti-angiogenic properties. Resveratrol has direct inhibitory action on cardiac fibroblasts and may inhibit the progression of cardiac fibrosis, which has beneficial cardiovascular effects. Resveratrol is considered a potential neuroprotective agent in treating focal cerebral ischemia injury, Huntington's disease, and Alzheimer's disease [46]. Recently, resveratrol was found to protect the spinal cord, kidney, and heart from ischemia-reperfusion injury through upregulation of NO [47]. Resveratrol has been reported to either suppress [48] or enhance NO production [49]. Resveratrol inhibits NOS activity and modifies iNOS expression [50]. Resveratrol may inhibit cell proliferation through the up-regulation of eNOS transcripts and the subsequent activation of p53 [51].

Resveratrol has several effects on retinal injury. Resveratrol reduces oxidation and proliferation of human retinal pigment epithelial cells via extracellular signal-regulated kinase inhibition [52]. Resveratrol exerts its antiproliferative effect on HepG2 hepatocellular carcinoma cells by inducing cell cycle arrest and NOS activation [53].

The mechanism by which resveratrol exerts its health-promoting effects is not yet fully elucidated in either *in vivo* or *in vitro* OIR. Our data showed that the expression of iNOS and/or mRNA in both *in vivo* and *in vitro* OIR according to administration of resveratrol was more reduced in the H group than in the N group and was increased in the HR group compared to the H group. However, the expression of eNOS and nNOS and/or mRNA was reverse as compared to those of iNOS. The data is similar to our previous report on the neuroprotective effects on hypoxic-ischemic encephalopathy [15]. In the present study, both *in vivo* and *in vitro* OIR revealed the same result, possibly because we used retinal cell enriched neurons.

In conclusion, resveratrol exerts some protective effects via modulation of NO-mediated mechanisms in both *in vivo* and *in vitro* OIR models.

Conflict of Interest

No potential conflict of interest relevant to this article was reported.

Acknowledgement

This work was supported by the grant of Research Institute of Medical Science, Catholic University of Daegu (2008).

References

1. Palmer EA, Flynn JT, Hardy RJ, et al. Incidence and early course of retinopathy of prematurity. The Cryotherapy for Retinopathy of Prematurity Cooperative Group. *Ophthalmology* 1991;98:1628-40.
2. Mantagos IS, Vanderveen DK, Smith LE. Emerging treatments for retinopathy of prematurity. *Semin Ophthalmol* 2009; 24:82-6.
3. Palmer EA, Hardy RJ, Dobson V, et al. 15-year outcomes following threshold retinopathy of prematurity: final results from the multicenter trial of cryotherapy for retinopathy of prematurity. *Arch Ophthalmol* 2005;123:311-8.
4. Good WV. Retinopathy of prematurity and the peripheral retina. *J Pediatr* 2008;153:591-2.
5. Heidary G, Vanderveen D, Smith LE. Retinopathy of pre-

maturity: current concepts in molecular pathogenesis. *Semin Ophthalmol* 2009;24:77-81.
6. Penn JS, Tolman BL, Lowery LA. Variable oxygen exposure causes preretinal neovascularization in the newborn rat. *Invest Ophthalmol Vis Sci* 1993;34:576-85.
7. Seigel GM. Establishment of an E1A-immortalized retinal cell culture. *In vitro Cell Dev Biol Anim* 1996;32:66-8.
8. Soleas GJ, Diamandis EP, Goldberg DM. Wine as a biological fluid: history, production, and role in disease prevention. *J Clin Lab Anal* 1997;11:287-313.
9. Creasy LL, Coffee M. Phytoalexin production potential of grape berries. *J Am Soc Hortic Sci* 1988;113:230-4.
10. Sun AY, Simonyi A, Sun GY. The "French Paradox" and beyond: neuroprotective effects of polyphenols. *Free Radic Biol Med* 2002;32:314-8.
11. Frankel EN, Waterhouse AL, Kinsella JE. Inhibition of human LDL oxidation by resveratrol. *Lancet* 1993;341:1103-4.
12. Shin NH, Ryu SY, Lee H, et al. Inhibitory effects of hydroxystilbenes on cyclooxygenase from sheep seminal vesicles. *Planta Med* 1998;64:283-4.
13. Bertelli AA, Giovannini L, Giannessi D, et al. Antiplatelet activity of synthetic and natural resveratrol in red wine. *Int J Tissue React* 1995;17:1-3.
14. Chen CK, Pace-Asciak CR. Vasorelaxing activity of resveratrol and quercetin in isolated rat aorta. *Gen Pharmacol* 1996;27:363-6.
15. Seo MA, Jang YY, Choi EJ, et al. The expression patterns of nitric oxide synthases (NOS) by resveratrol in hypoxic-ischemic brain injury in neonatal rat model. *Korean J Perinatol* 2008;19:283-92.
16. Lee HJ, Ju M, Park HJ, et al. The expression of nitric oxide synthase (NOS) isoforms in relation to Resveratrol administration in hypoxic injury of myocardial cells. *J Korean Pediatr Cardiol Soc* 2007;11:199-205.
17. Mosmann T. Rapid colorimetric assay for cellular growth and survival: application to proliferation and cytotoxicity assays. *J Immunol Methods* 1983;65:55-63.
18. Terry TL. Extreme prematurity and fibroblastic overgrowth of persistent vascular sheath behind each crystalline lens. *Am J Ophthalmol* 1942;25:203-4.
19. Terry TL. Fibroblastic overgrowth of persistent tunica vasculosa lentis in premature infants, II: report of cases-clinical aspects. *Arch Ophthalmol* 1943;29:36-53.
20. Owens WC, Owens EU. Retrolental fibroplasia in premature infants. *Am J Ophthalmol* 1949;32:1-29.
21. Kinsey VE. Retrolental fibroplasia; cooperative study of retrolental fibroplasia and the use of oxygen. *AMA Arch Ophthalmol* 1956;56:481-543.
22. Rubaltelli DM, Hirose T. Retinopathy of prematurity update. *Int Ophthalmol Clin* 2008;48:225-35.
23. Fleck BW, McIntosh N. Pathogenesis of retinopathy of prematurity and possible preventive strategies. *Early Hum Dev* 2008;84:83-8.
24. Hughes S, Yang H, Chan-Ling T. Vascularization of the human fetal retina: roles of vasculogenesis and angiogenesis. *Invest Ophthalmol Vis Sci* 2000;41:1217-28.
25. Leske DA, Wu J, Fautsch MP, et al. The role of VEGF and IGF-1 in a hypercarbic oxygen-induced retinopathy rat model of ROP. *Mol Vis* 2004;10:43-50.
26. Chen J, Smith LE. Retinopathy of prematurity. *Angiogenesis* 2007;10:133-40.
27. Cunningham S, Fleck BW, Elton RA, McIntosh N. Transcutaneous oxygen levels in retinopathy of prematurity. *Lancet* 1995;346:1464-5.
28. McColm JR, Cunningham S, Wade J, et al. Hypoxic oxygen fluctuations produce less severe retinopathy than hyperoxic fluctuations in a rat model of retinopathy of prematurity. *Pediatr Res* 2004;55:107-13.
29. Seigel GM. The golden age of retinal cell culture. *Mol Vis* 1999;5:4.
30. Politi LE, Adler R. Generation of enriched populations of cultured photoreceptor cells. *Invest Ophthalmol Vis Sci* 1986; 27:656-65.
31. Cahill GM, Besharse JC. Light-sensitive melatonin synthesis by Xenopus photoreceptors after destruction of the inner retina. *Vis Neurosci* 1992;8:487-90.
32. Wang X, Silverman M. A new technique for isolation of photoreceptor layer. *Zhonghua Yan Ke Za Zhi* 1996;32:304-6.
33. Seigel GM, Mutchler AL, Imperato EL. Expression of glial markers in a retinal precursor cell line. *Mol Vis* 1996;2:2.
34. Laabich A, Vissvesvaran GP, Lieu KL, et al. Protective effect of crocin against blue light- and white light-mediated photoreceptor cell death in bovine and primate retinal primary cell culture. *Invest Ophthalmol Vis Sci* 2006;47:3156-63.
35. Moncada S, Higgs A. The L-arginine-nitric oxide pathway. *N Engl J Med* 1993;329:2002-12.
36. Riddell DR, Owen JS. Nitric oxide and platelet aggregation. *Vitam Horm* 1999;57:25-48.
37. Konishi R, Shimizu R, Firestone L, et al. Nitric oxide prevents human platelet adhesion to fiber membranes in whole blood. *ASAIO J* 1996;42:M850-3.
38. Dal Secco D, Paron JA, de Oliveira SH, et al. Neutrophil migration in inflammation: nitric oxide inhibits rolling, adhesion and induces apoptosis. *Nitric Oxide* 2003;9:153-64.
39. Faraci FM, Brian JE Jr. Nitric oxide and the cerebral circulation. *Stroke* 1994;25:692-703.
40. Morikawa E, Moskowitz MA, Huang Z, et al. L-arginine infusion promotes nitric oxide-dependent vasodilation, increases regional cerebral blood flow, and reduces infarction volume in the rat. *Stroke* 1994;25:429-35.
41. Alderton WK, Cooper CE, Knowles RG. Nitric oxide synthases: structure, function and inhibition. *Biochem J* 2001; 357:593-615.
42. Tsai SK, Hung LM, Fu YT, et al. Resveratrol neuroprotective effects during focal cerebral ischemia injury via nitric oxide mechanism in rats. *J Vasc Surg* 2007;46:346-53.
43. Rotondo S, Rajtar G, Manarini S, et al. Effect of trans-resveratrol, a natural polyphenolic compound, on human polymorphonuclear leukocyte function. *Br J Pharmacol* 1998; 123:1691-9.
44. Aggarwal BB, Bhardwaj A, Aggarwal RS, et al. Role of resveratrol in prevention and therapy of cancer: preclinical and clinical studies. *Anticancer Res* 2004;24:2783-840.
45. Love S. Oxidative stress in brain ischemia. *Brain Pathol* 1999;9:119-31.
46. Huang SS, Tsai MC, Chih CL, et al. Resveratrol reduction of infarct size in Long-Evans rats subjected to focal cerebral ischemia. *Life Sci* 2001;69:1057-65.
47. Hattori R, Otani H, Maulik N, Das DK. Pharmacological preconditioning with resveratrol: role of nitric oxide. *Am J Physiol Heart Circ Physiol* 2002;282:H1988-95.
48. Chung EY, Kim BH, Lee MK, et al. Anti-inflammatory effect of the oligomeric stilbene alpha-Viniferin and its mode of the action through inhibition of cyclooxygenase-2 and inducible nitric oxide synthase. *Planta Med* 2003;69:710-4.
49. Wallerath T, Deckert G, Ternes T, et al. Resveratrol, a polyphenolic phytoalexin present in red wine, enhances expression and activity of endothelial nitric oxide synthase. *Circulation* 2002;106:1652-8.
50. Chan MM, Mattiacci JA, Hwang HS, et al. Synergy between ethanol and grape polyphenols, quercetin, and resveratrol, in the inhibition of the inducible nitric oxide synthase

pathway. *Biochem Pharmacol* 2000;60:1539-48.
51. Uchida Y, Yamazaki H, Watanabe S, et al. Enhancement of NF-kappaB activity by resveratrol in cytokine-exposed mesangial cells. *Clin Exp Immunol* 2005;142:76-83.
52. King RE, Kent KD, Bomser JA. Resveratrol reduces oxidation and proliferation of human retinal pigment epithelial cells via extracellular signal-regulated kinase inhibition. *Chem Biol Interact* 2005;151:143-9.
53. Notas G, Nifli AP, Kampa M, et al. Resveratrol exerts its antiproliferative effect on HepG2 hepatocellular carcinoma cells, by inducing cell cycle arrest, and NOS activation. *Biochim Biophys Acta* 2006;1760:1657-66.